

Large aperture, sparse pulse coded MIMO sonars, principles and performance

Oleksandr Malyuskin, Alex Noel Joseph Raj, David Cooper, Adrian McKernan

ECIT, Queen's University Belfast, Queen's Road, Belfast BT3 9DT, UK

Oleksandr Malyuskin, o.malyuskin@qub.ac.uk

Abstract: The operation principles of 2D and 3D large aperture, sparse multiple input multiple output (MIMO) sonars, their key imaging characteristics and processing speed will be discussed in this talk. These types of sonars can be applied in many ultrasonic imaging applications, including underwater target localisation, proximity sensing, and real-time underwater imaging. The study focuses on the operation of pulsed narrowband sonars using single or multiple orthogonal frequency bands, binary phase or pulse delay coding to achieve beamforming control in both transmit and receive modes. A particular emphasis is given to the sonar modes' inter-operability (for example, sequential Single Input Single Output, Multiple Input Single Output and full MIMO modes) and the effect of this interoperability on the underwater target(s) resolution, discrimination and processing speed. The mathematical model of imaging is based on the time-domain scattering amplitude calculation and echo signal processing using cross-correlation functions. The target(s) features extraction based on the cross-correlation function envelop shape is discussed with a brief experimental demonstration of the 2D with field-programmable-gate-array (FPGA) digital signal processing cores.

Keywords: MIMO sonar, sparse sonar, large aperture, underwater imaging, super-resolution

INTRODUCTION

Sonar imaging systems acquire information about the underwater imaging scene by transmitting acoustic signals and analyzing the echoes reflected from the underwater targets to estimate the targets' range, location, velocity and scattering strength. In this work, we analyse the performance characteristics of a high-frequency ($>40\text{kHz}$) active pulsed MIMO sonar operating in a single or multiple orthogonal narrowband frequencies.

In traditional single or multi-beam phased-array sonar systems, beam scanning in transmit mode is achieved through progressive time delay or phase difference between the adjacent transducers in the sonar array and coherent echo processing by the receivers [1]. A MIMO sonar can generate space-time waveform diversity both in transmit and receive modes resulting in various imaging scenarios improving target resolution and acquisition speed or enabling cognitive target detection and tracking [2]-[5].

The schematic diagram of a MIMO sonar under study is shown in Fig.1.

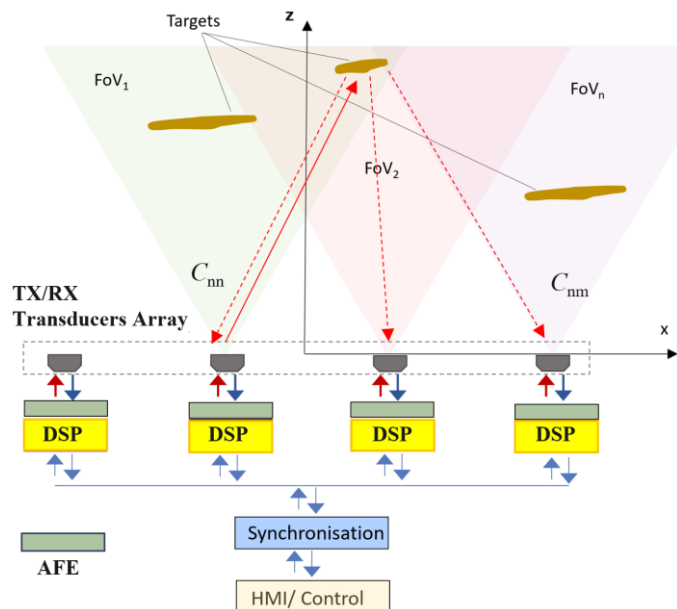


Fig.1: Schematic diagram of a MIMO sonar array. AFE – analog front-end, DSP- digital signal processing unit, TX and RX are the transmit and receive elements of the signal chain, FoV_n - field of view of the n -th sonar transducer.

MIMO diversity [6], [7] can be achieved through several techniques or their combination:

- MIMO modes interoperability
- Binary phase shift coding (BPSK)
- Pulse length and pulse delay coding
- Amplitude coding

Some of these features of MIMO sonar are discussed below.

MIMO SONAR BEAMFORMING

Acoustic pressure $p(\vec{r}, t)$ generated by a pulsed sonar transducer array can be written, for a single ping, in the following form

$$p(\vec{r}, t) = \sum_{n=1}^N \sum_{m=1}^M A_n \sin[2\pi f(t - \tau_n - R_n/v) + s_{mn}] F_p(t, \tau_n, T_m, T_n) \frac{F_n(\theta, \phi)}{4\pi R_n} \quad (1)$$

In Eq.(1), \vec{r} and \vec{r}_n are the radius vectors of the observation position and the centre of the n -th transducer respectively, A_n is a peak acoustic pressure level at the n -th transducer, f – centre frequency of the narrowband sinusoidal pulse, $R_n = |\vec{r} - \vec{r}_n|$, v is the speed of sound in the medium, $F_n(\theta, \phi)$ is an acoustic radiation pattern of the n -th transducer, Fig.2(a). Parameters s_{mn} define the BPSK symbols and parameters τ_n, T_m, T_n define the time delay of the n -th transducer pulse, m -th BPSK symbol length and the overall pulse length, respectively, generated by the n -th transducer, Fig.2(b).

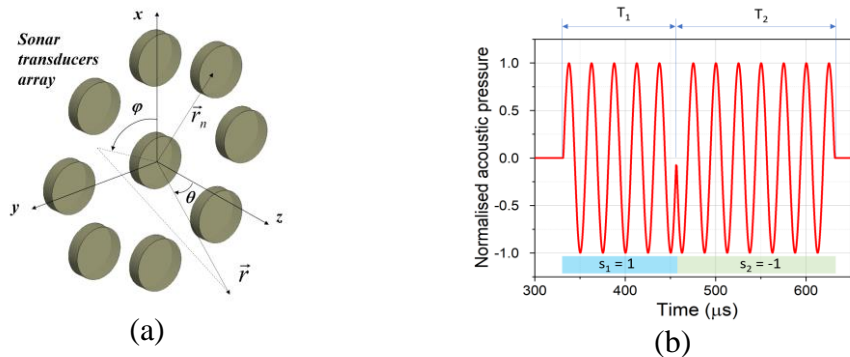


Fig.2: MIMO sonar array geometry parameters (a) and pulse waveforms (b). In Fig.2(b), the simulation of the 2-symbol acoustic pressure waveform is shown at a distance of 0.1 m from the transducer in the air.

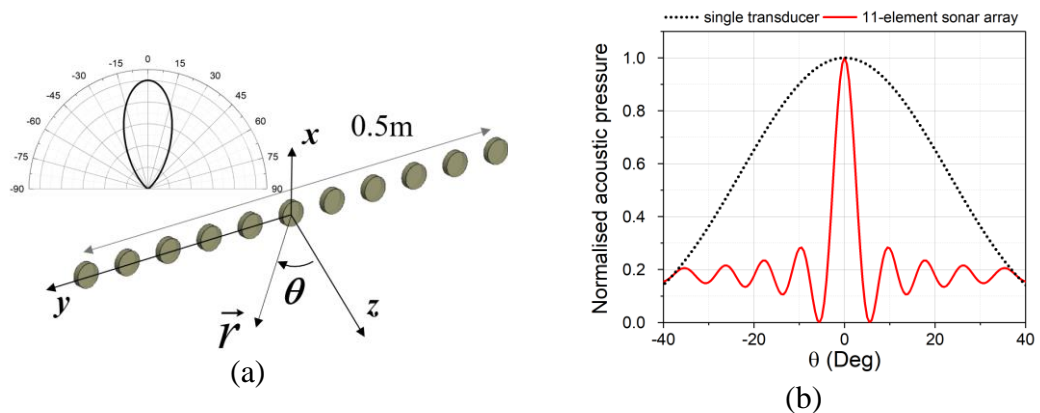


Fig.3: 2D sparse MIMO sonar model (a), operating as a forward-looking sonar in a deep water column at the centre frequency of 40kHz. (b) Radiation patterns of a single sonar transducer and an 11-element array under synchronous excitation.

The effect of spatial beam compression using sparse pulsed 2D sonar is shown in Fig. (3), (4).

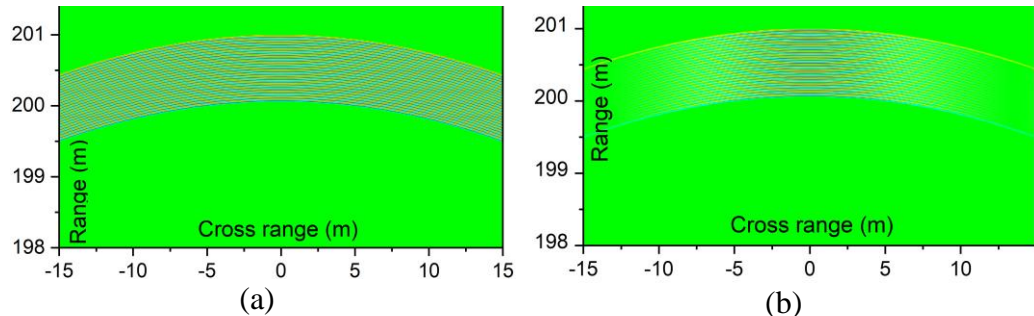


Fig.4: A far-field 2D acoustic pressure distribution of the pulsed sonar. (a) Single transducer pulse; (b) acoustic pulse of an 11-element sparse sonar, with all transducers synchronously excited by a 40kHz narrowband pulse.

In this simulation, the transducers with a 50° full beam angle (at 3dB) are excited synchronously at 40kHz. It can be seen that the far-field pattern of a sparse array is compressed 10 times in the angular range. For a wider field of view imaging, the scene can be scanned by the sequential firing of the transducers and when the target is detected, a narrow simultaneous firing could lead to a narrow field of view and finer cross-range resolution. The range resolution can be improved by utilising BPSK coding of the sonar pulse, using e.g. Barker codes [8].

TARGET DETECTION

In the MIMO imaging mode, the targets can be detected and characterised by processing the echo signals using cross-correlation functions C_{nm}

$$C_{nm}(\tau) = \int_{t_0}^{t_0+T} s_{TX_n}(t-\tau) s_{RX_m}(t) dt \quad (2)$$

Where s_{TX_n} is the signal generated by the n -th transducer signal in transmit mode and s_{RX_m} is a received signal by the m -th transducer in receive mode, Fig.1. The signal generation and echo processing (1), (2) results in the cross-correlation matrix, capturing all possible signal transmission paths between the targets in the imaging area and elements in the pulsed sonar array. In the second step, the time-of-flight and target cross-range characteristics in the sonar field of view can be established by processing the cross-correlation peak and envelop information thus extracting the target positions and respective cross-range information, Fig.5.

The processing time of target(s) detection and characterisation is defined as

$$t \approx 2 \cdot D_{\max} \cdot N_{mn} \quad (3)$$

Where D_{\max} is the maximum imaging range and N_{mn} is the number of pings by (m,n) combinations of transducers.

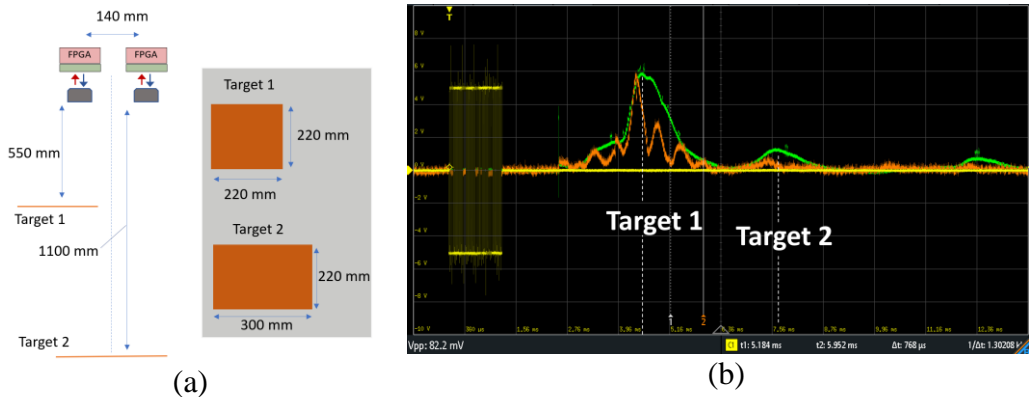


Fig.5: An experimental forward-looking sonar operation in the air environment
 (a) Imaging scene geometry; (b) 40kHz transmitted pulse with BPSK phase modulation (yellow line), and cross-correlation of received signals in monostatic (green line) and bistatic (orange line) modes.

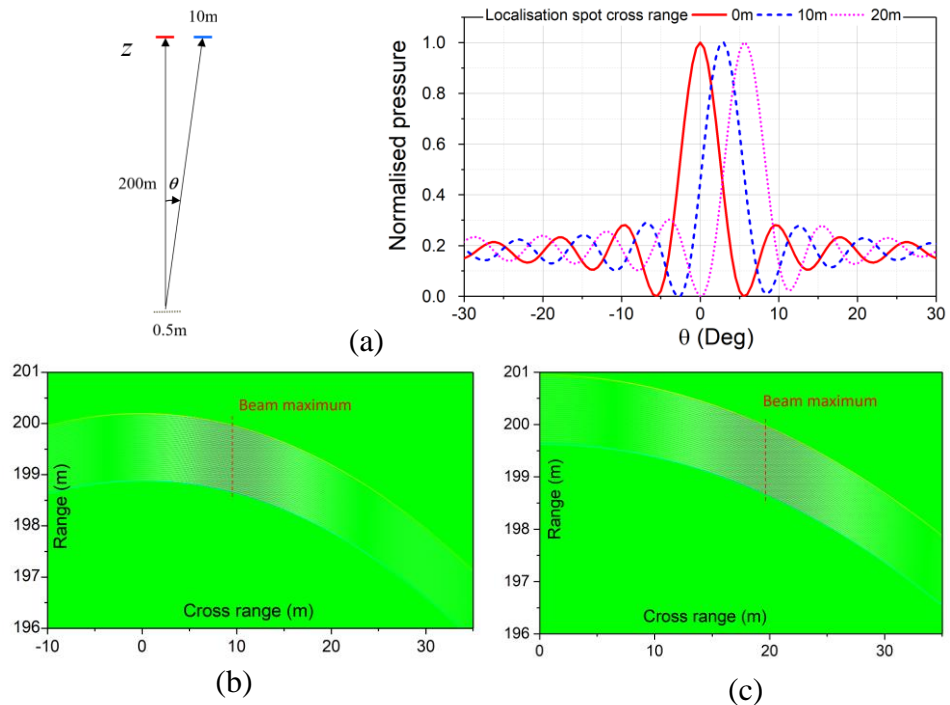


Fig.6: Time-delay beam localisation, full-wave simulation: (a) angular coordinates and 2D snapshots of localisation areas with the centres in (b) (10m, 200m), (c) (20m, 200m)

Depending on the sonar operating requirements, time delay or BPSK coding, or a combination of these techniques can be used to increase the signal-to-noise ratio at the receiver or increase range or cross-range resolution. Fig.6 illustrates time-reversal acoustic beamforming [9] using time delays for different localisation zones in the far field of 11-element 2D sonar of 0.5m aperture and transducers with $\Delta\theta_t = 50^\circ$ full beamwidth (at 3dB). It can be seen that an angular resolution of 3° (at 3dB) is possible with this array, which is better than $\sim\Delta\theta_t/N_A$, N_A is a number of elements.

CONCLUSIONS

Sparse pulsed MIMO sonar arrays offer several distinct advantages over the traditional phase scanning sonars, enabling fast (real-time) imaging, space-time beamforming diversity in both transmit and receive modes and lower complexity of digital signal processing hardware as compared to phase scanning sonars. The challenges of the sparse sonars are the relatively lower angular resolution ($\sim \Delta\theta_t/N_A$, $\Delta\theta_t$ is transducer angular beamwidth, N_A is a number of elements,) than is achievable in large phase scanning sonars, which can be compensated by BPSK and time delay coding and the requirement in a more complex image processing algorithms that will be discussed for several key underwater imaging scenarios in our future work.

ACKNOWLEDGEMENTS

This study was conducted as part of the Belfast Maritime Consortium UKRI Strength in Places project, ‘Decarbonisation of Maritime Transportation: A return to Commercial Sailing’ led by Artemis Technologies Ltd, Project no. 107138. The Authors thank Artemis Technologies Ltd.’s technical team (Dr Benoit Lecallard, Dr Emer McAleavy) and the SIP Programme Director Dr Katrina Thompson for continuous support and insightful technical discussions.

REFERENCES

- [1] **L. Bjørnø**, *Applied Underwater Acoustics*, Elsevier, 2017.
- [2] **I. Bekkerman and J. Tabrikian**, Target Detection and Localization Using MIMO Radars and Sonars, *IEEE Transactions on Signal Processing*, 54(10), 3873-3883, 2006.
- [3] **X. Liu**, et al., High-resolution two-dimensional imaging using MIMO sonar with limited physical size. *Applied Acoustics*, 182, 108280, 2021. <https://doi.org/10.1016/j.apacoust.2021.1082801>
- [4] **Y. Pailhas and Y. Petillot**, Neither PAS nor CAS: MIMO, *OCEANS 2016 - Shanghai*, China, 2016, 1-4, doi: 10.1109/OCEANSAP.2016.7485394.
- [5] **N. Sharaga**, et al., Optimal Cognitive Beamforming for Target Tracking in MIMO Radar/Sonar, *IEEE Journal of Selected Topics in Signal Processing*, 9(8), 1440-1450, 2015.
- [6] **W. Men**, et al., Waveform Design and Processing for Joint Detection and Communication Based on MIMO Sonar Systems, *5th Int. Conf. Inf. Comm. Signal Processing (ICICSP)*, Shenzhen, China, 2022, 523-527.
- [7] **Y. Pailhas**, et. al, Spatially Distributed MIMO Sonar Systems: Principles and Capabilities, *IEEE Journal of Oceanic Engineering*, 42(3), 738-751, 2017.
- [8] **R. Boucheron**, Over-sampling improvement for acoustic triangulation using Barker code audio signals. *Proc. Mtgs. Acoust*, 30 (1): 070005, 2017.
- [9] **H. Zhou** et.al., Enhanced target detection in clutter using dispersive delay lines and time reversal, *Electronic Letters*, 50(20), 1480-1482, 2014.